

## Crystal structure of cobalt molybdate hydrate $\text{CoMoO}_4 \cdot n\text{H}_2\text{O}$

Kazuo Eda<sup>a,\*</sup>, Yuichi Uno<sup>a</sup>, Noriko Nagai<sup>a</sup>, Noriyuki Sotani<sup>a</sup>, M. Stanley Whittingham<sup>b</sup>

<sup>a</sup>Faculty of Science, Department of Chemistry, Kobe University, Nada-ku, Kobe 657-8501, Japan

<sup>b</sup>Institute for Materials Research, State University of New York at Binghamton, Binghamton, NY 13902-6000, USA

Received 6 May 2005; received in revised form 7 June 2005; accepted 11 June 2005

Available online 20 July 2005

### Abstract

We have determined the crystal structure of the title compound, which has a triclinic cell with cell parameters of  $a = 6.844 \text{ \AA}$ ,  $b = 6.933 \text{ \AA}$ ,  $c = 9.339 \text{ \AA}$ ,  $\alpha = 76.617^\circ$ ,  $\beta = 84.188^\circ$ ,  $\gamma = 74.510^\circ$  and space group  $P\bar{1}$ . The crystal structure suggests the chemical formula  $\text{CoMoO}_4 \cdot 3/4\text{H}_2\text{O}$ . The structure consists of  $\text{MoO}_4$  tetrahedra and  $\text{CoO}_6$  octahedra, confirming the earlier X-ray absorption near-edge spectroscopic (XANES) investigation on the hydrate. The comparison of the crystal structures of the hydrate and the  $\alpha$ -,  $\beta$ -, and  $hp$ -phases shows that the hydrate exhibits metal cation coordinations similar to those of the  $\beta$ -phase, but had arrangements of  $\text{CoO}_6$  and  $\text{MoO}_n$  polyhedra similar to those of the  $hp$ -phase.

© 2005 Elsevier Inc. All rights reserved.

**Keywords:** Crystal structure; Cobalt molybdate; Oxide hydrate;  $\text{CoMoO}_4 \cdot n\text{H}_2\text{O}$

### 1. Introduction

Cobalt molybdates are attractive compounds because of their structural, magnetic, and catalytic properties [1–9]. They are especially important components of industrial catalysts. Their catalytic properties are closely related to their structure [5,7]. Four compounds with the  $\text{CoMoO}_4$  stoichiometry are known: the low temperature  $\alpha$ -phase (pale green, space group:  $C2/m$ ;  $a = 9.67$ ,  $b = 8.85$ ,  $c = 7.76 \text{ \AA}$ ,  $\beta = 113.49^\circ$ ) [10], the high temperature  $\beta$ -phase (pale violet,  $C2/m$ ;  $a = 10.21$ ,  $b = 9.31$ ,  $c = 7.01 \text{ \AA}$ ,  $\beta = 106.4^\circ$ ) [2,11], the high-pressure ( $hp$ -) phase (black,  $P2/c$ ,  $a = 4.6598$ ,  $b = 5.6862$ ,  $c = 4.9159 \text{ \AA}$ ,  $\beta = 90.521^\circ$ ) [4], and the hydrate (violet, crystal structure: unknown up to now). The hydrate has been known to directly transform into the  $\beta$ -phase when it entirely loses its crystallization water at around 600 K. This transformation occurs at much lower temperature than the transition from  $\alpha$ - to  $\beta$ -phase (ca. 750),

and is probably facilitated by the structural similarities of the hydrate and  $\beta$ -phase [8]. Recently, we have found another direct transformation of the hydrate into the  $hp$ -phase under hydrothermal conditions, which transformation will be presented elsewhere. In order to understand not only these transformations but also their catalytic or physical properties, comparison of their structures is necessary. The crystal structures of three out of the four compounds (except the hydrate) are known as mentioned above. It is only suggested that the hydrate consists of  $\text{CoO}_6$  and  $\text{MoO}_4$  polyhedra according to X-ray absorption near-edge spectroscopic (XANES) investigation [8].

In order to reveal the structure of the hydrate, we succeeded in preparing a single crystal of it. The single crystal analysis confirmed that the hydrate consists of  $\text{CoO}_6$  and  $\text{MoO}_4$  polyhedra, and the polyhedra in the hydrate are connected similarly to that in the  $hp$ -phase rather than those in  $\alpha$ - and  $\beta$ -phases. In the present paper we will present the structure of the hydrate and compare it with the structures of the  $\text{CoMoO}_4$  phases.

\*Corresponding author. Fax: +81 78 803 5677.

E-mail address: [eda@kobe-u.ac.jp](mailto:eda@kobe-u.ac.jp) (K. Eda).

## 2. Experimental

### 2.1. Preparation of the hydrate

0.720 g of  $\text{MoO}_3$  (5 mmol) and 0.375 g of  $\text{CoO}$  (5 mmol), were suspended in 30 ml of distilled water. 0.292 g of  $\text{NaCl}$  (5 mmol) was added to the solution in order to increase the ionic strength of the solution and promote crystal growth of the hydrate during the hydrothermal treatment. Then the solution was put into a 60 ml Teflon-lined autoclave and heated in a forced convection oven at 453 K under autogenous pressure (ca. 10 atm) for 1 day. The resulting product was filtered, washed with distilled water, and dried in air at room temperature. Even without the addition of  $\text{NaCl}$  a single phase product of the hydrate was obtained and confirmed by powder X-ray diffraction, but no crystals sufficient for single crystal X-ray analysis were grown in spite of varying treatment temperature (up to 473 K), treatment time, as well as the concentrations of  $\text{MoO}_3$  and  $\text{CoO}$ .

### 2.2. Crystal structure determination of the hydrate

Single crystal diffraction data were collected on a Bruker smart 1000 diffractometer with a CCD detector using graphite monochromated  $\text{MoK}\alpha$  radiation. The structure of the single crystal was solved by direct method and refined by full-matrix least-squares calculations based on  $F_o^2$  with empirical absorption corrections using Bruker SHELXTL programs.

### 2.3. Characterization of the hydrate

Powder X-ray diffraction (XRD) patterns of the samples were measured using a Bruker AXS MXP3VZ X-ray diffractometer with  $\text{CuK}\alpha$  radiation. Simulation of the diffraction pattern was calculated using Rietan 2000 [12]. The compositions of the products were analyzed by a HITACHI 180–80 atomic absorption spectrometer. TG-DTA analysis was performed on a Bruker AXS TG-DTA 2010 system at a heating rate of 10 K/min.

## 3. Results and discussion

### 3.1. Crystal structures of the hydrate

In order to determine the crystal structure of the hydrate, some crystals obtained were used for collecting diffraction data. All crystals used exhibited non-merohedral twinning, which rotated the reciprocal axes  $180^\circ$  about the  $a^* + c^*$  axis. Two distinct cell sets were separated using RLATT, identified using SMART (Bruker, 2001) and integrated using SAINT (Bruker,

Table 1  
Crystal data and structure refinement

Empirical formula	$\text{CoMoO}_4 \cdot 3/4\text{H}_2\text{O}$
Formula weight	232.38
Crystal system, space group	Triclinic, $P\bar{1}$
$a, b, c/\text{\AA}$	6.844(2), 6.933(2), 9.339(2)
$\alpha, \beta, \gamma/^\circ$	76.617(3), 84.188(7) 74.510(8)
$V/\text{\AA}^3, Z$	415.1(2), 4
Temperature/K	293(2)
Calculated density/ $\text{g cm}^{-3}$	3.758
$\mu/\text{mm}^{-1}$	6.912
$F(000)$	436
Crystal dimensions/ $\text{mm}^3$	$0.19 \times 0.04 \times 0.03$
$\theta$ range for data collection degrees	2.27–27.43
Limiting indices	$-8 \leq h \leq 8, -8 \leq k \leq 8, 0 \leq l \leq 11$
Reflections collected	1569
Independent reflections	1569
Restraints, parameters	0, 77
$R_1(F)$	0.0704
$wR_2(F^2)$	0.1748
	$w = 1/[\sigma^2(F_o^2) + (0.1013P)^2 + 0.0000P]$ where $P = (F_o^2 + 2F_c^2)/3$
CSD no.	415282

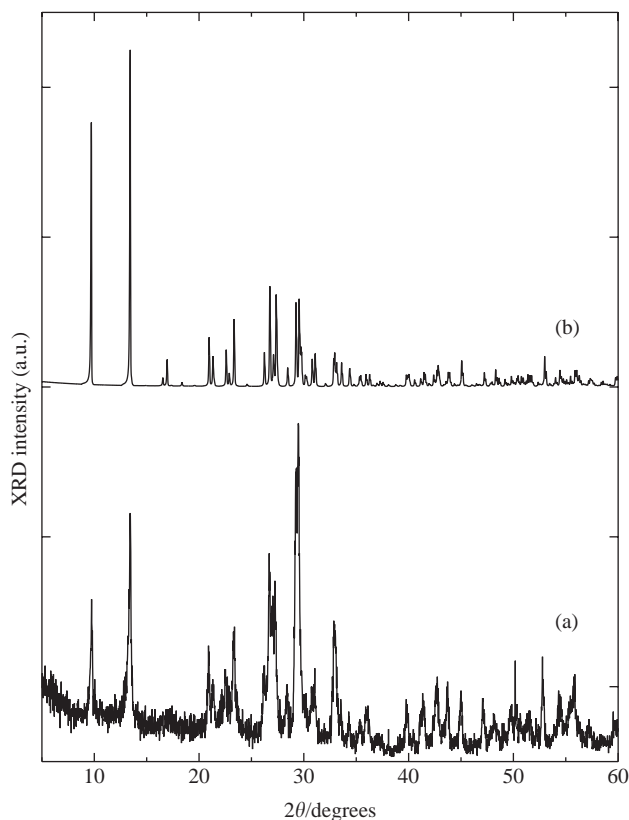


Fig. 1. Powder XRD patterns of the hydrate: measured (a) and simulated (b).

2001). The combined data were refined with separate scale factors using SHELXTL. The resulting crystal data and refinement for the hydrate are shown in Table 1. A triclinic cell with cell parameters of  $a = 6.844 \text{ \AA}$ ,  $b = 6.933 \text{ \AA}$ ,  $c = 9.339 \text{ \AA}$ ,  $\alpha = 76.617^\circ$ ,  $\beta = 84.188^\circ$ ,  $\gamma = 74.510^\circ$  was obtained, which made indexing of the powder diffraction pattern of the hydrate difficult. The powder XRD pattern simulation based on the present crystal data reproduced well the peak positions of the XRD patterns observed for polycrystalline samples of the hydrate obtained in the present work (Fig. 1) and in the literature [8]. Tables 2 and 3 show the atomic parameters and selected interatomic distances, respectively. Oxygen atoms were refined with isotropic displacement factors to avoid giving non-positive definite answers. The  $\text{O9}_{\text{cw}}$  is suggested to be an aqua

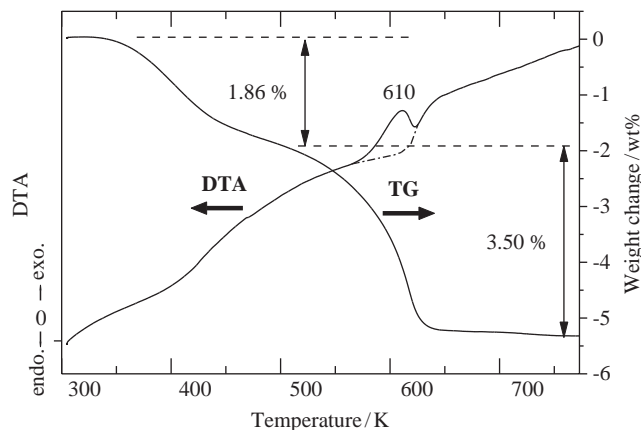


Fig. 2. TG-DTA curves in  $\text{N}_2$  of the hydrate.

Table 2

Atomic coordinates ( $\times 10,000$ ), equivalent isotropic displacements ( $\text{\AA}^2 \times 1000$ ), and bond valence sums (BVS)

Atom <sup>a</sup>	Site	Occupancy	x	y	z	$U_{\text{eq}}$	BVS
Co1	2i	1.0	1542(3)	6464(3)	6992(2)	11(1)	2.08
Co2	2i	1.0	1961(3)	8287(3)	9728(2)	9(1)	2.14
Mo1	2i	1.0	59(2)	1935(2)	6845(1)	11(1)	5.91
Mo2	2i	1.0	2482(2)	2943(2)	10,522(1)	9(1)	6.02
O1	2i	1.0	1446(14)	-720(14)	7475(11)	14(2)	1.96
O2	2i	1.0	1573(15)	3643(16)	6741(12)	21(2)	1.93
O3	2i	1.0	-824(16)	2209(16)	5124(10)	23(2)	2.01
O4	2i	1.0	-2105(14)	2633(15)	8022(11)	15(2)	1.80
O5	2i	1.0	2056(14)	5466(15)	9299(11)	16(2)	1.98
O6	2i	1.0	1285(15)	1367(15)	9836(12)	16(2)	2.12
O7	2i	1.0	1590(14)	3092(15)	12,306(12)	18(2)	1.92
O8	2i	1.0	5049(14)	1893(15)	10581(11)	18(2)	2.08
$\text{O9}_{\text{cw}}$	2i	1.0	4686(16)	5953(16)	6313(12)	25(3)	0.33
$\text{O10}_{\text{hw}}$	2i	0.5	-4570(60)	-140(60)	5430(40)	72(11)	0.04

<sup>a</sup>See Fig. 3 for atomic numbering.

Table 3

Selected interatomic distances ( $\text{\AA}$ )

Co1 octahedron		Co2 octahedron		Inter-cation <sup>a</sup>	
Co1–O2	2.018(11)	Co2–O8	2.012(10)	Co1–Co2	3.169(3)
Co1–O3	2.026(11)	Co2–O4	2.054(10)	Co1–Mo1	3.583(2)
Co1–O1	2.088(10)	Co2–O5	2.069(10)	Co1–Mo1	3.629(3)
Co1–O5	2.139(11)	Co2–O6	2.087(10)	Co1–Mo1	3.684(3)
Co1–O7	2.139(10)	Co2–O1	2.092(10)	Co1–Mo2	3.418(2)
Co1–O9	2.141(11)	Co2–O6	2.177(10)	Co1–Mo2	3.620(2)
				Co2–Co2	3.159(2)
Mo1 tetrahedron		Mo2 tetrahedron		Co2–Mo1	3.338(2)
Mo1–O3	1.726(11)	Mo2–O8	1.714(10)	Co2–Mo1	3.342(2)
Mo1–O2	1.752(10)	Mo2–O7	1.732(10)	Co2–Mo2	3.413(2)
Mo1–O4	1.781(9)	Mo2–O6	1.781(10)	Co2–Mo2	3.532(2)
Mo1–O1	1.819(9)	Mo2–O5	1.822(10)	Co2–Mo2	3.588(2)
				Co2–Mo2	3.665(2)
				Mo1–Mo2	4.233(2)
				Mo1–Mo2	4.351(2)
				Mo1–Mo2	3.851(2)

<sup>a</sup>All inter-cation distances  $< 4.5 \text{ \AA}$  are given.





dehydrations (at 350–450 and 500–620 K) as mentioned in the literature [8]. The former dehydration is reversible, and ascribed to lattice water. The latter is irreversible and accompanied with an exotherm at 610 K, which is superimposed on the broad intrinsic endotherm, shown with an additional one-point dotted line in the figure, due to the desorption. This dehydration leads to the transformation of the hydrate into  $\beta$ -CoMoO<sub>4</sub> and was attributed to coordination water. The weight losses of 1.86% and 3.50% due to the dehydrations correspond to  $n_{lw} = 0.24$  and  $n_{cw} = 0.45$ , respectively, and agree with the formula of CoMoO<sub>4</sub> · 3/4H<sub>2</sub>O ( $n = n_{lw} + n_{cw} = 3/4$ , where  $n_{lw} = 0.25$  and  $n_{cw} = 0.5$ ). This suggestion supports the above results, concerning coordination and lattice waters, of single crystal X-ray structure analysis.

Table 3 shows that the hydrate consists of MoO<sub>4</sub> tetrahedra and CoO<sub>6</sub> octahedra, and proves the presence of MoO<sub>4</sub> tetrahedra and CoO<sub>6</sub> octahedra in the hydrate, which has been suggested from XANES investigations [8]. Fig. 3 shows a polyhedral representation of the crystal structure of the hydrate, together with the structures of the other three CoMoO<sub>4</sub> phases. In the hydrate the lattice water occupies the disordered sites around (0.5 0.0 0.5), as mentioned above, but is omitted in the figure for clarity. According to the figure four CoO<sub>6</sub> octahedra constitute a tetramer ( $z$ -shaped) [CoO<sub>6</sub>]<sub>4</sub> unit sharing edges. The  $z$ -shaped [CoO<sub>6</sub>]<sub>4</sub> units are linked with MoO<sub>4</sub> tetrahedra to form the three-dimensional oxide network.

The hydrate has a lower density (3.76 g/cm<sup>3</sup>) than the  $\alpha$ - (4.78 g/cm<sup>3</sup>),  $\beta$ - (4.57 g/cm<sup>3</sup>) and  $hp$ - (5.58 g/cm<sup>3</sup>) phases. Thus its unit cell has large cavities, one of which is occupied by the lattice water (O10<sub>lw</sub>). These cavities spread around a line linking the lattice positions (0.50 0.0 0.5) and (0.5 1.0 0.5). Hydrogen atoms of the coordination water (O9<sub>cw</sub>) are projecting into the cavities. Such structural features might be related to its

high catalytic activity for hydrosulfurization, compared with other CoMoO<sub>4</sub> phases [7,13].

### 3.2. Comparison of the structures

Fig. 3 shows that all the four compounds contain CoO<sub>6</sub> octahedra. These octahedra form two types of  $z$ -shaped [CoO<sub>6</sub>]<sub>4</sub> units depending on the compounds, although the units in the  $hp$ -phase are not isolated like those in the other three compounds. One is a condensed type of unit that is represented by joining two dimers of edge-shared CoO<sub>6</sub> octahedra with a discrepancy of a half width of the octahedra, which is found in the  $\alpha$ - and  $\beta$ -phases (Fig. 3(b) and (c)). The other is a lengthened type of unit that is built by joining two dimers with a discrepancy of one and a half width of the octahedra, and is in the hydrate and the  $hp$ -phase (Fig. 3(a) and (d)). Thus the hydrate exhibits the coordination of the Co atom similar to those of the other three phases, and has the further similarity in the connecting manner of the octahedra with the  $hp$ -phase.

As for the MoO<sub>n</sub> polyhedra, both tetrahedra (MoO<sub>4</sub>) and octahedra (MoO<sub>6</sub>) are observed depending on the compound. Octahedra are found in the  $\alpha$ - and  $hp$ -phases, and are directly linked by sharing edges to form two types of  $z$ -shaped [MoO<sub>6</sub>]<sub>4</sub> units depending on the compounds. A condensed type of unit is formed in the  $\alpha$ -phase (Fig. 3(b)), whereas a lengthened type of unit, in the  $hp$ -phase (Fig. 3(d)). Tetrahedra are found in the  $\beta$ -phase and the hydrate, and are not directly linked with each other, but are located as if they constitute virtual [MoO<sub>4</sub>]<sub>4</sub>  $z$ -shaped units. Fig. 4 shows the detailed arrangements of the MoO<sub>n</sub> polyhedra in the real and virtual [MoO<sub>n</sub>]<sub>4</sub>  $z$ -shaped units observed in the four compounds [4,10,14,15]. The virtual unit in the  $\beta$ -phase (Fig. 4(c)) has dihedral symmetry and the two Mo atoms at both ends of the unit are located symmetrically against the two central Mo atoms ( $d_A:d_B = 4.19:4.19$ )

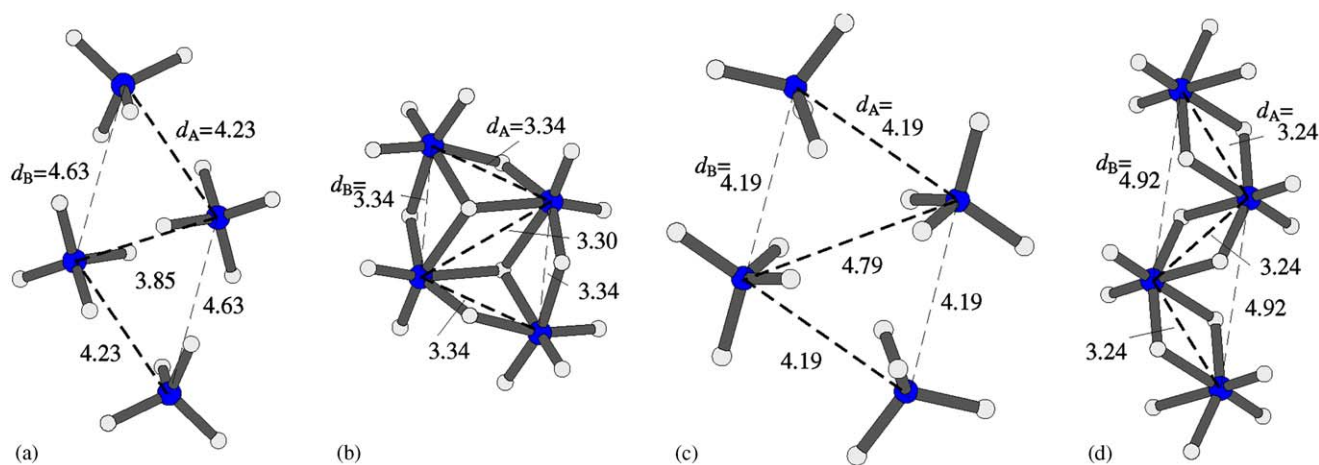


Fig. 4. Polyhedral configurations in the real and virtual  $z$ -shaped [MoO<sub>n</sub>]<sub>4</sub> units: hydrate (a),  $\alpha$ -phase (b),  $\beta$ -phase [13] (c), and  $hp$ -phase (d). Separations among neighboring Mo atoms are presented in Å.

like those in the real condensed unit of the  $\alpha$ -phase ( $d_A:d_B = 3.34:3.34$ ). Thus, it is regarded as a virtual condensed type of unit. In the hydrate the two terminal Mo atoms are located not symmetrically against the central atoms (that is, the ratio ( $d_A:d_B = 4.62:4.21$ ), and form a virtual lengthened type of unit (Fig. 4(a)). Thus,

the hydrate has a coordination of the Mo atom similar to that in the  $\beta$ -phase, but the arrangements of the  $\text{MoO}_n$  polyhedra are similar to those in the *hp*-phase.

According to the above results the hydrate exhibits the coordinations of the metal cations similar to those of the  $\beta$ -phase, and has arrangements of  $\text{MO}_n$  ( $M = \text{Co}$ ,

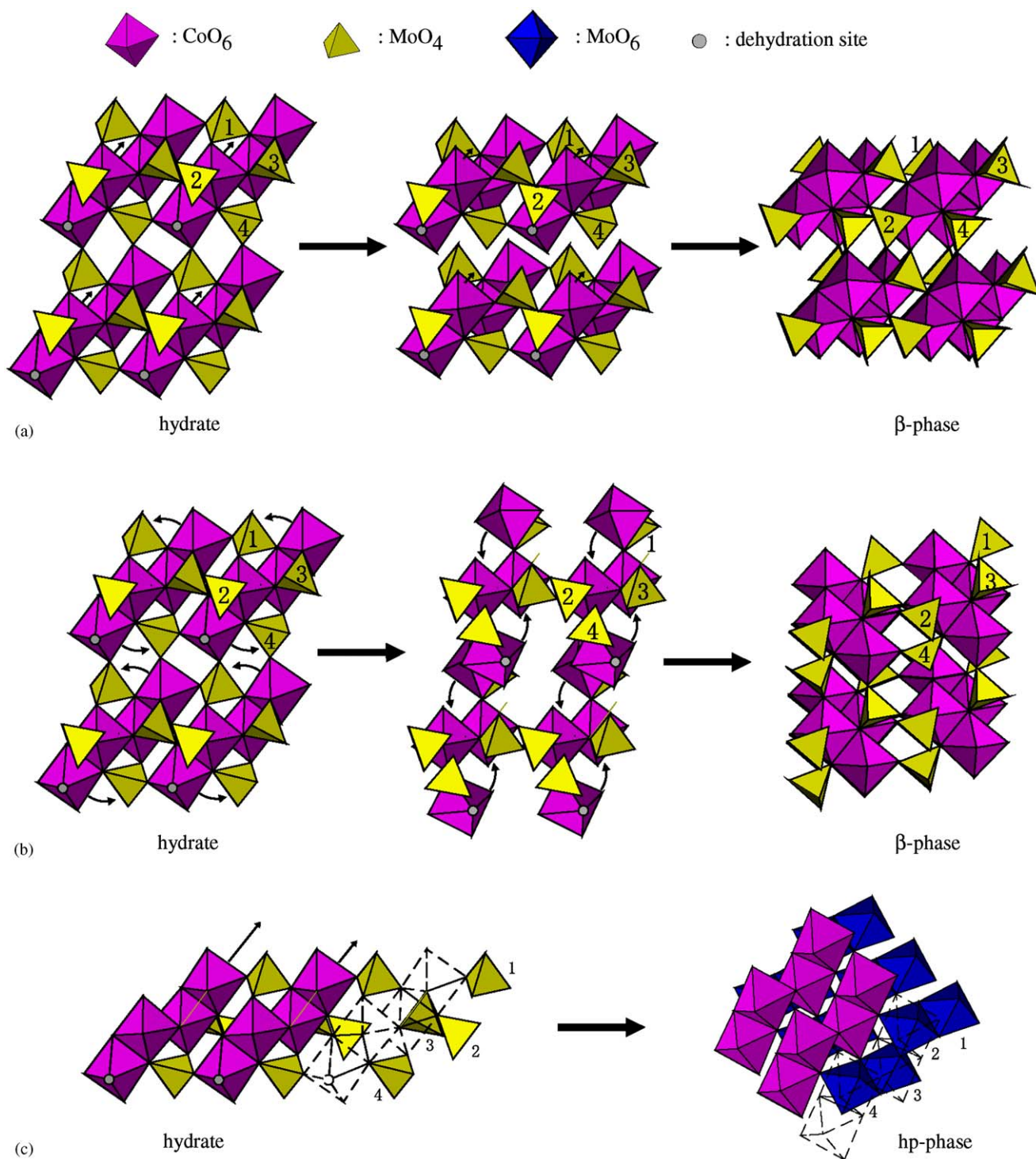


Fig. 5. Hypothetical mechanisms of the structural transformations: from hydrate to  $\beta$ -phase mainly with translational displacements (a), from hydrate to  $\beta$ -phase mainly with rotational displacements (b), and from hydrate to *hp*-phase mainly with translational displacements (c).

Mo) polyhedra similar to those of the *hp*-phase. Such structural similarities allow hypothetical transformations of the hydrate into the  $\beta$ - and *hp*-phases by simple translational or rotational displacements of corresponding polyhedra, as shown in Fig. 5. Thus the real direct transformations can be achieved at lower temperatures.

### Acknowledgments

The authors thank Dr. Masao Hashimoto for his valuable discussion. The work at Binghamton was supported by the National Science Foundation Grant 0313963.

### References

- [1] A.P. Young, C.M. Schwartz, *Science* 141 (1963) 348.
- [2] A.W. Sleight, B.L. Chamberland, *Inorg. Chem.* 7 (1968) 1672.
- [3] M. Wiesmann, H. Ehrenberg, G. Wltschek, P. Zinn, H. Weitzel, H. Fuess, *J. Magn. Magn. Mater.* 150 (1995) L1.
- [4] C. Livage, A. Hynaux, J. Marot, M. Nogues, G. Férey, *J. Mater. Chem.* 12 (2002) 1423.
- [5] C. Mazzocchia, C. Aboumradi, C. Diagne, E. Tempesti, J.M. Herrmann, G. Thomas, *Catal. Lett.* 10 (1991) 181.
- [6] J. Zou, G.L. Schrader, *J. Catal.* 161 (1996) 667.
- [7] J.L. Brito, A.L. Barbosa, *J. Catal.* 171 (1997) 467.
- [8] J.A. Rodriguez, S. Chaturvedi, J. Hanson, A. Albornoz, J.L. Brito, *J. Phys. Chem. B* 102 (1998) 1347.
- [9] J.A. Rodriguez, S. Chaturvedi, J. Hanson, A. Albornoz, J.L. Brito, *J. Phys. Chem. B* 103 (1999) 770.
- [10] G.W. Smith, J.A. Ibers, *Acta Cryst.* 19 (1965) 269.
- [11] P. Courtine, P.P. Cord, G. Pannetier, J.C. Daumas, R. Montarnal, *Bull. Soc. Chim. Fr.* (1968) 4816.
- [12] F. Izumi, T. Ikeda, *Mater. Sci. Forum* 321–324 (2000) 198.
- [13] F.E. Massoth, in: D.D. Eley, H. Pines, P.B. Weisz (Eds.), *Advances in Catalysis*, vol. 27, 1978, p. 302.
- [14] For the  $\beta$ -phase the atomic positions have not been presented yet. The separations among neighbor Mo atoms in this phase were evaluated using the atomic positions of  $\alpha$ -MnMoO<sub>4</sub> [15], which is isostructural with  $\beta$ -CoMoO<sub>4</sub>.
- [15] S.C. Abrahams, J.M. Reddy, *J. Chem. Phys.* 43 (1965) 2533.